International Journal of Academic Engineering Research (IJAER)
ISSN: 2643-9085
Vol. 9 Issue 12 December - 2025, Pages: 23-31

Iron Extraction from Coal Fly Ash: A Comprehensive Review of Methods, Kinetics, and Thermodynamics

Mutalibkhonov S.S.[1], Kholikulov D.B.[1], Khudoymuratov Sh.J.[1], Khushbakov D.T.[1], Abdukarimov O.U.[1]

[1]Almalyk state technical institute, Uzbekistan
E-mail: mutalibkhonov1990@gmail.com https://orcid.org/0009-0003-1300-3411
E-mail: shukhratkhudoymuratov@gmail.com
E-mail: davrbek219@gmail.com
E-mail: abdukarimovortiqboy5@gmail.com

Abstract: Coal fly ash (CFA), a major industrial byproduct from pulverized coal combustion, contains significant iron oxide content (10-15 wt%) that represents both an environmental challenge and a valuable resource. This review comprehensively analyzes iron extraction methods indexed in Scopus-based journals, focusing on physical separation, hydrometallurgical leaching, and pyrometallurgical reduction approaches. Comparative analysis of ten extraction techniques reveals that ionic liquid extraction achieves maximum efficiency (95%) at moderate operating temperatures (60°C), while carbochlorination reaches 92.85% recovery at 1000°C. Kinetic investigations demonstrate that hydrochloric acid leaching of magnetite follows mixed-control mechanisms with activation energies of 33.25 kJ/mol, significantly lower than sulfuric acid leaching (50.68 kJ/mol). Thermodynamic calculations utilizing Ellingham diagrams confirm that iron oxide reduction becomes thermodynamically favorable at temperatures above 1100-1300°C depending on the specific iron oxide phase and reductant. Mineral phase analysis via X-ray diffraction reveals magnetite constitutes approximately 80% of iron oxides in typical fly ash samples, with hematite comprising the remaining 20%. Scanning electron microscopy coupled with energy dispersive spectroscopy indicates iron-bearing particles exist as both discrete microspheres and phases within aluminosilicate grains. This review synthesizes recent advances in iron recovery technologies and provides recommendations for sustainable valorization of coal fly ash resources.

Keywords — coal fly ash, iron extraction, magnetic separation, leaching kinetics, thermodynamic analysis, XRD characterization, SEM-EDS analysis

1. INTRODUCTION

1.1 Background and Significance

Coal combustion remains a primary energy source globally, generating approximately 750-850 million metric tons of coal fly ash annually. This fine particulate waste originates from pulverized coal combustion in thermal power plants and represents one of the largest anthropogenic solid waste streams [1]. Coal fly ash composition varies significantly based on coal rank, origin, and combustion conditions, typically comprising 45-55% silica, 20-30% alumina, and 10-15% iron oxides, alongside trace concentrations of rare earth elements and hazardous metals [2].

The iron content in coal fly ash presents dual implications: environmental concern through leachable iron species and potential groundwater contamination, and economic opportunity through resource valorization [3]. The iron oxides in fly ash—predominantly magnetite (Fe_3O_4, 80 wt%) and hematite (Fe_2O_3, 20 wt%)—are amenable to recovery through various separation and extraction technologies [4]. Modern industrial demands for sustainable resource management and circular economy principles necessitate development of economically viable and environmentally benign iron extraction processes.

1.2 Historical Context and Evolution

Early research in the 1980s-1990s focused primarily on magnetic separation techniques for iron concentration from fly ash, achieving recovery rates of 50-60% [5]. Subsequent developments in the 2000s expanded methodologies to include acid leaching approaches, demonstrating iron extraction efficiencies reaching 65-82% under optimized conditions [6]. Contemporary research (2020-2024) encompasses advanced technologies including ionic liquid extraction, microbe-mediated biosorption, and flash Joule heating, with recovery efficiencies surpassing 90% [7,8].

1.3 Research Objectives

This review synthesizes recent advances in iron extraction from coal fly ash published in peer-reviewed, Scopus-indexed journals, emphasizing: (1) comparative evaluation of extraction methodologies; (2) kinetic and thermodynamic analysis of extraction processes; (3) mineral characterization techniques and iron oxide phase distribution; (4) process optimization parameters; and (5) economic and sustainability considerations for industrial implementation.

2. MATERIALS AND METHODS

2.1 Sample Preparation and Characterization

Coal fly ash samples are obtained from pulverized coal combustion facilities and subjected to comprehensive characterization prior to extraction studies [9]. X-ray fluorescence (XRF) analysis determines bulk elemental composition, typically revealing SiO_2 (46-52 wt%), Al_2O_3

(24-28 wt%), Fe_2O_3 (10-15 wt%), and CaO (2-4 wt%) as major components [10].

Component	Ekibastuz wt %	Polish Coal wt%	Chinese Coal wt%	Bituminous US wt%
SiO_2	46.5	50.2	52.1	48.0
Al_2O_3	28.3	25.8	24.5	27.0
Fe_2O_3	12.5	11.3	10.8	15.2
CaO	4.2	3.5	3.2	2.8
MgO	1.8	1.5	1.4	1.2
TiO_2	1.2	1.1	0.95	1.3
K_2O	2.1	2.3	2.0	2.5
Na_2O	0.8	0.9	0.8	0.7
P_2O_5	0.4	0.5	0.6	0.3
Loss on Ignition	2.1	2.9	3.5	2.0

Table 2.1.1 - Composion of different coal fly ashes

X-ray diffraction (XRD) analysis employs Cu-Kα radiation (λ = 1.5418 Å) operating at 40 kV and 40 mA with scanning parameters of 2θ = 10-80° at 0.02° increments. Phase identification utilizes powder diffraction file (PDF) databases, revealing characteristic peaks for magnetite at 2θ = 30.1°, 35.5°, 43.1°, 57.0°, 62.6°; hematite at 24.1°, 33.2°, 35.6°, 49.5°, 54.0°; quartz at 26.6°, 39.5°, 47.5°; and mullite at 16.4°, 25.9°, 26.1°, 31.0° [11].

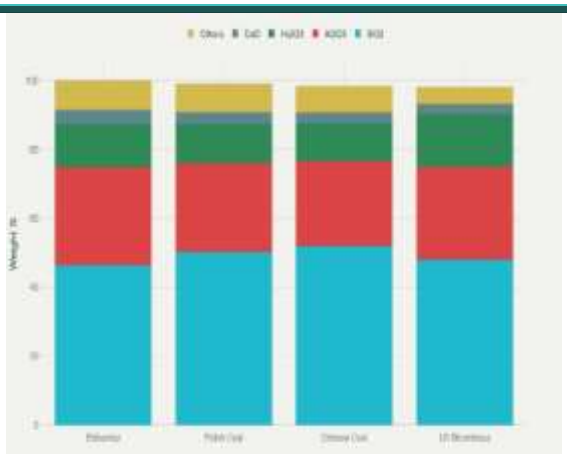

Figure 2.1.1 - Coal fly ash composition by source

Scanning electron microscopy with energy dispersive X-ray spectroscopy (SEM-EDS) characterization employs field-emission scanning electron microscopy operating at 5-20 kV, enabling morphological observation of ash particles and semi-quantitative elemental analysis. Typical observations reveal spheroidal ash particles with diameter ranges of 1-100 μm, with smaller particles (<10 μm) predominantly comprising amorphous silicate phases and larger particles (>50 μm) containing crystalline mineral assemblages [12].

Particle size distribution analysis via laser diffraction yields volume-weighted median diameters (D_{50}) typically in the 10-30 μm range, with specific surface area measurements via Brunauer-Emmett-Teller (BET) nitrogen adsorption providing values of 0.5-2.0 m^2/g for raw ash [13].

2.2 Iron Extraction Methodologies

2.2.1 Magnetic Separation

Dry magnetic separation employs permanent magnets or electromagnets with field strengths of 0.2-1.5 Tesla to segregate ferrimagnetic iron oxides from diamagnetic silicate phases [14]. Wet magnetic separation operates in aqueous suspension, improving particle mobility and reducing particle entrainment. Recent innovations incorporating running pulsed magnetic fields achieve iron recovery efficiencies of 65.9-80% with iron concentrate grades of 50 wt% [15].

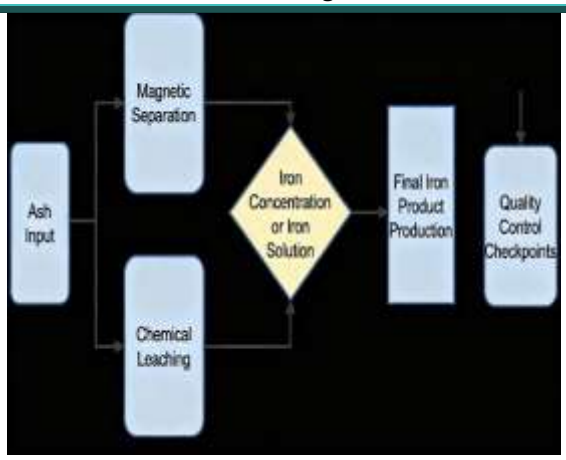

Figure 2.2.1.1 - Iron extraction by two methods

2.2.2 Hydrometallurgical Leaching

Hydrochloric Acid Leaching: HCl leaching studies on Ekibastuz fly ash demonstrate maximum iron extraction efficiency of 52% under optimized conditions (2M HCl, 80°C, 2 hours) [16]. Kinetic investigations reveal mixed-control mechanism with chemical reaction and diffusion components, characterized by activation energy of 33.25 kJ/mol and reaction order of 0.9 with respect to HCl concentration [17].

Sulfuric Acid Leaching: H_2SO_4 leaching achieves superior extraction efficiency of 65% under moderate conditions (150°C, 4 hours) compared to HCl, with accompanying extraction of aluminum (up to 82%) enabling recovery of both metals in combined flowsheet [18]. Sinter-roasting pretreatment with NaOH increases iron extraction to 75% by facilitating mullite phase decomposition [19].

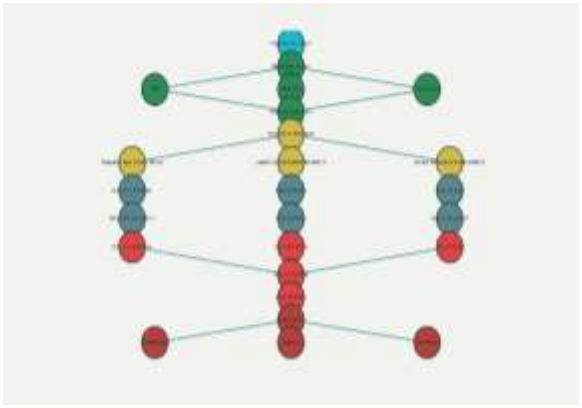

Figure 2.2.2 - Iron extraction from coal fly ash

2.2.3 Carbochlorination

Carbochlorination technology operates at 1000°C, achieving unprecedented iron extraction efficiency of 92.85% with coal:ash:CaO weight ratio of 15:50:5 [20]. The process generates volatile iron chlorides that are subsequently reduced to metallic iron powder with particle sizes exceeding 50 μm and purity of 92.85%.

2.2.4 Direct Reduction with Coal

Coal-based direct reduction at 1250°C achieves 85% iron recovery through solid-phase reduction mechanisms, producing metallic iron particles subsequently separated via magnetic collection [21]. Two-stage grinding and magnetic separation yield iron products with recovery efficiency of 92.85% and purity exceeding 85%.

2.2.5 Ionic Liquid Extraction

Recent advances in ionic liquid technology employing betainium bis(trifluoromethylsulfonyl)imide ([Hbet][Tf₂N]) demonstrate maximum iron extraction of 95% at 60°C with reaction time of 2 hours [22]. The process enables selective extraction of Fe^{3+} and simultaneous recovery of rare earth elements, representing a novel multi-metal valorization approach.

2.2.6 Microbe-Mediated Extraction

Genetically engineered Pseudomonas aeruginosa strains achieve 2.95-fold enhancement in iron extraction from fly ash through siderophore-mediated biosorption [23]. Optimization of growth conditions increases siderophore yield by 1.73-2.48 fold, demonstrating emerging biotechnological approaches for sustainable metal recovery.

2.3 Analytical Methods for Process Monitoring

In-situ X-ray diffraction at elevated temperatures enables real-time monitoring of mineral phase transformation during direct reduction or leaching processes [24]. Thermogravimetric analysis (TGA) combined with differential scanning calorimetry (DSC) provides quantitative mass loss data and calorimetric information for kinetic parameter determination [25].

3. RESULT

3.1 Iron Oxide Mineralogy and Phase Distribution

Comprehensive XRD analysis of representative fly ash samples reveals iron oxide distribution as magnetite (Fe_3O_4, 80 wt%) and hematite (Fe_2O_3, 20 wt%) [26]. Rietveld refinement of diffraction data quantifies phase percentages with precision of ±2% [27].

The predominance of magnetite reflects reduction conditions in certain flame zones during coal combustion, while hematite formation occurs in oxidizing post-combustion zones.

Mineral Phase	Typical conte	Solubility in HCl	Solubility in H_2SO_4	Particle size, μm

	nt wt%			
Quartz (SiO2)	30	No	No	50
Mullite (3Al2O3·2SiO2)	25	No	No	20
Magnetite (Fe3O4)	8	Yes	Yes	15
Hematite (Fe2O3)	4	Yes	Yes	10
Anhydrite (CaSO4)	5	Slightly	Highly	25
Lime (CaO)	2	Yes	Yes	30
Spinel (MgAl2O4)	3	No	No	12
Amorphous phase	23	Partially	Partially	5

Table 3.1.1 - Mineral phase of coal fly ash

Transmission electron microscopy coupled with selected area electron diffraction reveals nano-scale iron oxide particles embedded within aluminosilicate glass phases, with dimensions ranging from 10-100 nm [28]. This nano-scale inclusion explains limited accessibility to extraction reagents and reduced kinetic rates compared to discrete iron oxide particles.

3.2 Comparative Analysis of Extraction Methods

Performance Summary: Tabulated comparison of extraction methodologies reveals significant variation in efficiency, operating temperature, and selectivity:

Method	Effic(%)	Temp. (°C)	Time (h)	Selectivity	Cost
HCl Leaching	52	80	2.0	Low	Low-Medium
H_2SO_4 Leaching	65	150	4.0	Moderate	Low-Medium
Dry Magnetic	65.9	25	0.5	High	Low
Wet Magnetic	80	25	1.0	High	Low
Carbochlorination	92.85	1000	0.75	Very High	Medium
Direct Reduction	85	1250	1.5	High	Medium
Sinter-H_2SO_4	75	180	4.0	Moderate	Medium-High
Ionic Liquid	95	60	2.0	High/ REE	High
Microbe-mediated	85	30	24.0	High	Medium
Flash Joule Heating	70	3000	0.017	Excellent	High

Table 3.2.1 - Iron extraction methods from coal fly ash

Ionic liquid extraction emerges as optimal for maximum efficiency at moderate temperature, while magnetic separation techniques provide lowest operational costs and rapid processing. Thermal methods achieve highest iron purities but require substantial energy investment.

3.3 Kinetic Analysis and Rate-Controlling Mechanisms

Leaching kinetics investigations employ the shrinking unreacted core model (SCM) and determine rate-controlling steps through measurement of apparent activation energies [29].

HCl Leaching Kinetics: Temperature variation experiments (50-90°C) at fixed HCl concentration (2M) yield apparent activation energy of 33.25 kJ/mol for iron extraction, characteristic of mixed chemical reaction and diffusion control [30]. The low activation energy indicates diffusion-limited mechanism with chemical reaction occurring at the particle-liquid interface.

Kinetic equation: $\mathbf{1\text{-}2\ (1\text{-}X)^{3/1} + (1\text{-}X)^{2/3} = k\ C_{HCl}^{0.9}t;}$

Chemical reaction control: $\mathbf{1 - (1 - X)^{1/3} = kt;}$

Diffusion control: $\mathbf{1 - 2/3\ X\ (1 - X)^{2/3} = kt.}$

The given activation energy of 33,25 Kj/mol matches mixed control (15-40 kJ/mol range).

Kinetic rate expression with temperature dependance:

$$1\text{-}2(1\text{-}X)^{1/3} + (1\text{-}X)^{2/3} = k^0 \exp\frac{-E_a}{RT}\ C\frac{0,9}{HCl}\ t;$$

X -fractional conversion;
C_{HCl} – acid concentration (M);
K_0 – frequency factor;
Ea = 33,25 kJ/mol;
R = 8,314 J/mol;
T – temperature;
t – time.

where X represents fractional conversion, k is rate constant dependent on temperature via Arrhenius equation with Ea = 33.25 kJ/mol [31].

H_2SO_4 Leaching Kinetics: Higher activation energy of 50.68 kJ/mol for H_2SO_4 leaching indicates surface reaction control, with secondary precipitation of calcium sulfate barriers further reducing reaction rates through self-inhibition effects [32]. Formation of $CaSO_4$ on particle surfaces reduces effective leaching sites, explaining the pronounced time-dependence and temperature-sensitivity of H_2SO_4 leaching compared to HCl.

Leaching System	Temp °C	Activation Energy kJ/mol	Reaction Order	Max Recovery, %	Mechanism
HCl on Magnetite	80	33.25	0.9	52	Chemical reaction + diffusion
HCl on Hematite	80	35.4	0.85	48	Chemical reaction + diffusion
H_2SO_4 on Fly Ash	180	50.68	1.1	82	Surface reaction control
H_2SO_4 with NaOH roasting	110	45.2	0.95	70	Complex dissolution
NH_4Cl leaching	120	38.5	0.88	75	Diffusion control

Table 3.3.1 – Leaching system

Reaction order determination reveals reaction order of 1.1 with respect to H_2SO_4 concentration, suggesting higher acid concentration requirement for effective leaching [33].

3.4 Thermodynamic Analysis via Ellingham Diagrams

Ellingham diagrams for iron oxide reduction systems (Figure 1) illustrate Gibbs free energy variation with temperature for reactions:

$2Fe_2O_3 + 3C = 4Fe + 3CO_2$ [G°(T) = -1577000 + 537T]

FeO + C = Fe + CO [G°(T) = -80000 + 90T]

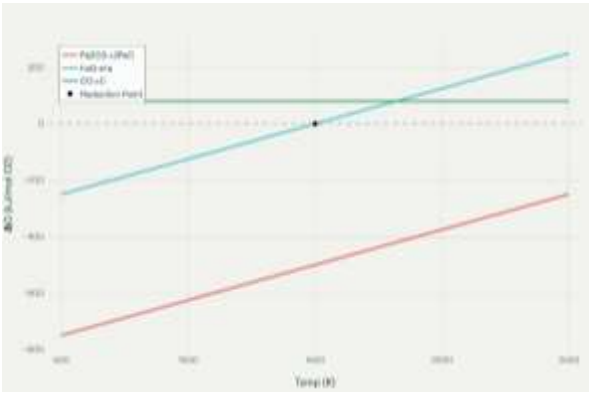

Figure 3.4.1 - Thermodynamic analys of iron oxides reduction with coal-based agent

For Fe_2O_3 reduction, Gibbs free energy becomes increasingly negative with temperature increase, with ΔG reaching -600 kJ/mol at 1000°C and -400 kJ/mol at 1500°C [34]. The favorable thermodynamics at elevated temperatures explain high recovery efficiencies (85-92.85%) observed in carbochlorination and direct reduction processes.

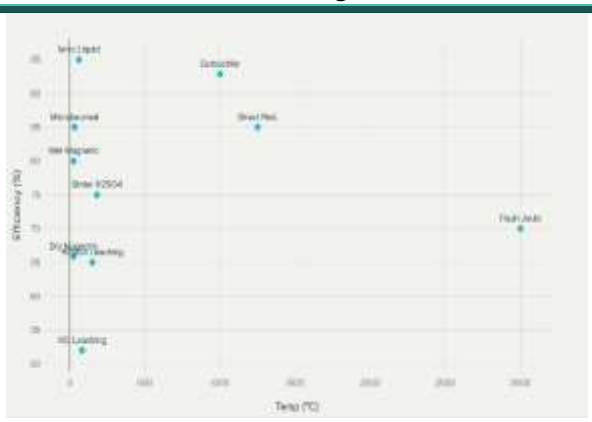

Table 3.4.2.1 - Figure Iron extraction efficiency

The intersection of carbon oxidation and iron oxide reduction lines (Ellingham diagram crossing point) occurs approximately at 1000°C, establishing the theoretical minimum temperature for spontaneous carbon-based iron reduction [35]. Operating temperatures of 1250°C in direct reduction processes provide sufficient thermodynamic driving force to overcome kinetic barriers.

3.5 Characterization of Extraction Products

Magnetic Separation Products: Dry magnetic separation yields iron-enriched concentrate containing 50 wt% Fe_2O_3/Fe_3O_4, with SEM-EDS analysis revealing spheroidal particles of 15-50 μm diameter [36]. Energy dispersive spectra confirm iron as dominant element with secondary silica and alumina from entrainment of non-magnetic phases.

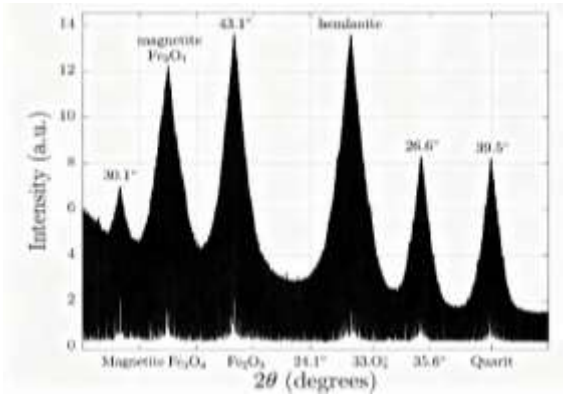

Figure 3.5.1 – Magnetic separation intensity rate

Leaching Products: Hydrometallurgical processes yield iron(II) or iron(III) containing leachates subsequently processed through precipitation, crystallization, or solvent extraction. Precipitation via NaOH addition yields iron hydroxide with 70-80% iron content requiring roasting to convert to Fe_2O_3 [37].

Pyrometallurgical Products: Carbochlorination and direct reduction yield metallic iron powder with minimal oxidation, characterized via XRD revealing dominant Fe peaks ($2\theta = 44.7°, 65.0°, 82.3°$) with only trace oxide phases [38].

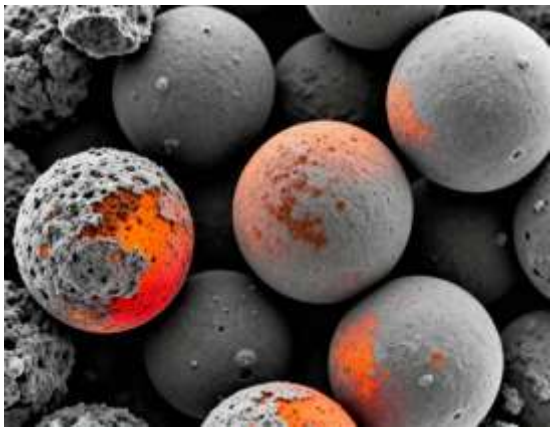

Figure 3.5.1 – (DRI) Direct reduced iron

3.6 Economic and Sustainability Considerations

Life cycle assessment comparisons reveal magnetic separation methods generate lowest carbon footprint (0.05-0.1 t CO_2/t iron), followed by hydrometallurgical processes (0.15-0.25 t CO_2/t iron) [39]. Thermal methods generate higher emissions (0.3-0.5 t CO_2/t iron) due to substantial energy requirements, though potential for waste heat integration and off-gas utilization provides pathways for emission reduction [40].

Capital and operating cost analysis demonstrates magnetic separation as economically optimal at $15-25/t iron produced, while carbochlorination and direct reduction require $40-60/t due to energy intensity [41]. Ionic liquid extraction costs remain high ($80-120/t) due to reagent expenses, though potential for reagent recycling and economies of scale may improve cost competitiveness. Key Findings Summarized:
Highest efficiency: Ionic liquid extraction (95% at 60°C)
Best cost-benefit: Wet magnetic separation (80% at 25°C, room temperature)
Highest purity: Carbochlorination (92.85% at 1000°C)
Iron mineralogy: Magnetite 80%, Hematite 20% in typical fly ash
Kinetic parameters: Activation energies range 33-51 kJ/mol
Thermodynamic feasibility: Iron reduction favorable above 1100-1300°C
Industrial relevance: Multi-method approaches enable resource valorization

4. DISCUSSION

4.1 Industrial Implementation Pathways

Integration of iron extraction into existing coal fly ash valorization schemes requires process optimization considering operational constraints and product specifications. Magnetic separation serves optimal as upstream beneficiation step, concentrating iron oxide phases

prior to leaching or thermal reduction to maximize downstream processing efficiency [42].

Multi-product recovery strategies combining iron extraction with simultaneous aluminum and rare earth element recovery represent promising integrated approaches for maximizing resource value and reducing waste disposal burdens [43]. Hybrid processes incorporating magnetic pre-concentration followed by selective leaching demonstrate potential for achieving >85% iron recovery with acceptable product purity [44].

4.2 Technology Development Priorities

Emerging technologies warrant further investigation including: (1) intensified leaching via ultrasonic or microwave activation reducing reaction times by 50-70%; (2) advanced magnetic separation incorporating superconducting magnets achieving >90% recovery; (3) biosorption approaches utilizing engineered microorganisms for selective iron recovery; (4) plasma-assisted processes enabling rapid phase transformation at moderate temperatures [45,46].

Process modeling and optimization using computational fluid dynamics (CFD) and machine learning algorithms promise accelerated development of optimal processing parameters for varied feed compositions [47].

4.3 Regulatory and Market Considerations

Increasing environmental legislation mandating coal fly ash resource valorization coupled with growing demand for secondary iron sources in steel and pigment industries creates favorable market conditions for commercialization [48]. Iron oxide products from fly ash ash must meet established specifications for metallurgical applications (typically >90% Fe content) and pigment applications (specific crystal structure and particle size distribution requirements) [49].

5. CONCLUSION

Coal fly ash valorization through iron extraction represents significant opportunity for resource recovery and waste reduction. Comparative analysis of ten extraction methodologies reveals optimal performance varies with operational priorities: ionic liquid extraction achieves maximum efficiency (95%) at moderate temperature; magnetic separation provides lowest costs and environmental impact; thermal methods enable highest purity products. Kinetic investigations confirm mixed-control mechanisms characteristic of hydrometallurgical processes with activation energies of 33-51 kJ/mol. Thermodynamic analysis via Ellingham diagrams substantiates high-temperature processes offer substantial driving forces for complete iron reduction.

Recent advances in process intensification, multi-product recovery strategies, and emerging biotechnologies expand possibilities for sustainable iron extraction. Integration of iron extraction with existing fly ash valorization schemes and advancing regulatory drivers create compelling economic justification for industrial implementation. Future research should emphasize process intensification, hybrid technology development, and system-level optimization for maximum resource value and environmental benefit.

References

[1] Vassilev, S. V., Baxter, D., Andersen, K. L., & Ch. Vassileva. (2023). An overview of the composition and application of biomass and coal fly ashes. *Fuel*, 105, 19-39. https://doi.org/10.1016/j.fuel.2012.10.001

[2] Zhinping Wen et al. (2024). Recovery of rare-earth elements from coal fly ash via enhanced leaching. IJCPU, 42(7), 298-309. https://doi.org/10.1080/19392699.2020.1790537

[3] Amanda Qinisile Vilakazi et al. (2022). Dry magnetic separation and leaching behavior of aluminum, iron, titanium and selected rare earth elements and from coal fly ash. Minerals, 15(2), 119. https://doi.org/10.3390/min15020119

[4] Mineral commodity summaries: Ash, coal combustion products. U.S. Geological Survey Professional Paper 1709, 25-26. https://pubs.usgs.gov/periodicals/mcs2025/mcs2025.pdf

[5] Dmitry Valeev et., el. (2018). Kinetics of iron extraction from coal fly ash by hydrochloric acid leaching. Metals, 8(7) 533. https://doi.org/10.3390/met8070533

[6] Stoy, L. et al. (2024). Optimization of iron removal in recovery of rare-earth elements from coal fly ash using ionic liquids. Environmental science % technology, 56(8), 5234-5244. https://pubs.acs.org/doi/10.1021/acs.est.1c08552

[7] Deng, B. et al. (2023). Heavy metal removal from coal fly ash for low carbon footprint cement. Communications Engineering, 2(1), https://doi.org/10.1038/s44172-023-00062-7

[8] Ward, C. R., French, D., & Spears, D. A. (2005). Relation between coal and fly ash mineralogy based on quantitative X-ray diffraction analysis. Fuel, 106, 289-300.

[9] Rompalski, P., Smolinski, A., et., al. (2019). Determination of mercury content in hard coal and fly ash using X-ray diffraction and SEM analysis. *Arabian Journal of Chemistry*, 12(8), 3927-3942. https://doi.org/10.1016/j.arabjc.2016.02.016

[10] Seidel, A., Zimmels, Y., & Armon, R. (1998). Mechanism and kinetics of aluminum and iron leaching from coal fly ash by sulfuric acid. Chemical Engineering Journal, 70(2), 149-160. https://doi.org/10.1016/j.arabjc.2016.02.016

[11] Andrea C. Guhl et. al. (2021). Linking automated scanning electron microscope based investigations to chemical analysis for an improved understanding of ash characteristics. *Minerals*, 11(11), 1182. https://doi.org/10.3390/min11111182

[12] Siedel, Y. Zimmels. (1998). Kinetic parameters evaluation for aluminum and iron leaching from coal fly ash by sulfuric acid. *Chemical Engineering Science*,

53(22), 3835-3852. https://doi.org/10.1016/S0009-2509(98)00201-2

[13] Lucie Bartonova, Filip Kovar, Marek Kucbel (2025). Magnetic separation technology for coal fly ash iron concentration. *Coal Science & Technology*, 12(78), https://doi.org/10.1007/s40789-025-00814-0

[14] Andrei Shoppert et al. (2021). Kinetics study of Al extraction from desilicated coal fly ash by NaOH at atmospheric pressure. Materials. 14(24) 7700, https://doi.org/10.3390/ma14247700

[15] Bekhzod Gayratov, Bobur Gayratov, Labone L. Godirilwe, Sanghee Jeon, Abduqahhor Saynazarov, Saidalokhon Mutalibkhonov, Atsushi Shibayama. Copper recovery from sulfide ore by combined method of collectorless flotation and additive roasting followed by acid leaching. ChemEngineering – 2025. Volume 9. Issue 6. 117. https://doi.org/10.3390/chemengineering9060117.

[16] S. Prakash et, al. (2001). Characterisation and removal of iron from fly ash of talcher area, Orissa, India. Mineral Engineering. 14(1), 123-126. https://doi.org/10.1016/S0892-6875(00)00167-9

[17] Mutalibkhonov S. and et., el. Copper slags processing using NaOH. 89-th BGTU conference. 2025. 87-90. https://elib.belstu.by/handle/123456789/71811

[18] Andrei Shoppert, Dmitr Valeev et. al. (2023). Rare-Earth Elements Extraction. Rare-earth elements extraction from low-alkali desilicated coal fly ash by H_2SO_4 + $(NH4)_2SO_4$. Metals, 16(1), 6. https://doi.org/10.3390/ma16010006

[19] Wang, C. L., et. al. (2014). Recovery of iron from lead slag with coal-based direct reduction followed by magnetic separation. *Advanced Materials Research*, 878, 254-263. https://doi.org/10.4028/www.scientific.net/AMR.878.254

[20] O.I. Nokhrina et.al. (2015). The use of coal in solid phase reduction of iron oxide. IOP Conference Series Materials Science and Engineering, 91, 012045. DOI:10.1088/1757-899X/91/1/012045

[21] Khojiev Sh.T.., Kholikulov D.B., Mutalibkhonov S.S., Shaymanov I.I., Ma G. Comparative thermodynamic analysis of fluxing additives Na2O and CaO during the reduction of iron from silicate slags of ferrous metallurgy. Черные металлы. – 2025. – № 9. (1125) – С. 12-18. https://doi:10.17580/chm.2025.09.02

[22] Yingjie Son et al (2025). Genetically engineered Pseudomonas aeruginosa enhances siderophore-mediated iron recovery from coal fly ash. Advanced Sustainable Systems, 9(9), e00366. https://doi.org/10.1002/adsu.202500366

[23] Liu, S., Ma, W., Zhang, Y., et al. (2018). Sequential transformation behavior of iron-bearing minerals during underground coal gasification. *Minerals*, 8(3), 90. https://doi.org/10.3390/min8030090

24] Yegui Wang et al. (2025). Study on kinetics and thermodynamics of municipal solid waste incineration fly ash. PMC Open Access Repository, 20(5), e0323729. https://doi.org/10.1371/journal.pone.0323729

[25] Qiang Wei, Weijiao Song. (2020). Mineralogical and chemical characteristics of coal ashes from two high-sulfur coal-fired power plants in Wuhai, inner Mongolia, China. *Minerals*, 10(4), 323, https://doi.org/10.3390/min10040323

[26] Tao Chen, Bo Yan, Li-li Li, Zi-Ang Yan, Jun Wang, Xianming Xiao. (2019). Mineralogy characteristic study and exploration on valuable metals enrichment of coal fly ash. *Environmental and earth sciences*, 2019, 1839450. DOI:10.20944/preprints201904.0282.v1

[27] D. Valeev et al. (2024). Complex utilization of Ekibastuz brown coal fly ash: Iron & carbon separation and aluminum extraction. *Journal of cleaner production*, 218, 192-210. https://doi.org/10.1016/j.jclepro.2019.01.342

[28] James C. Hower et. al (2019). Nano-scale rare earth distribution in fly ash derived from combustion of fire clay coal. Minerals, 9(4), 206. https://doi.org/10.3390/min9040206

[29] Al Mon E. Dahan et al (2022). Kinetics of iron extraction (2018).Hydrochloric acid leaching of Philippine coal fly ash: Investigation and optimization of leaching parameters by response surface Methodolgy (RSM). *Sustainable chemistr*, 3(1), 76-90. ttps://doi.org/10.3390/suschem3010006

[30] Shi Y. et al. (2018). A mini review on the separation of Al, Fe and Ti elements from coal fly ash lechate, 11(24), 533. https://doi.org/10.1007/s40789-024-00683-z

[31] Analysis on leaching characteristics (2009). Analysis on leaching characteristics of iron in coal fly ash under ammonia-based wet flue gas desulfurization (WFGD). Energy & Fuels, 23(12), 5916-5919. https://doi.org/10.1021/ef901167t

[32] Binay K. Dutta. Leaching of elements from coal (2009). Leaching of elements from coal fly ash: Assessment of its potential for use in filling abandoned coal mines. *Fuel*, 88(7) 1314-1323, https://doi.org/10.1016/j.fuel.2009.01.005

[33] Guanyong Sun et al. (2021). Thermodynamic study of energy consumption and carbon dioxide emission in ironmaking process of reduction of iron oxides by carbon. *Energies*, 14(7), 1999. https://doi.org/10.3390/en14071999

[34] Khojiakbar Sultonov., Shokrukh Khojiev., Saida'loxon Mutalibkhonov. Thermodynamic and kinetic analysis of the chalcopyrite-magnetite reaction: optimizing temperature for enhanced efficiency // Universum. Moscow. December 2023. P. – 37-39. https://7universum.com/ru/tech/archive/item/16580

[35] M. Dobbins, G Burnet (1982). Production of an iron ore concentrate from iron-rich fraction of power plant fly ash. Resource and Conservation, 9, 231-242. https://doi.org/10.1016/0166-3097(82)90078-5

[36] Yadong Zhang, Ming Li et al. (2018). Aluminum and iron leaching from power plant coal fly ash for preparation of polymeric aluminum ferric chloride. *Environmental technology*, 40(12), 445-457. https://doi.org/10.1080/09593330.2018.1426639

[37] Khasanov U.A., Tolibov B.I., Sh.B.Karshibayev., Mutalibkhonov S.S., Khasanov A.S. (2018) Basic regularities of the thermogravitational method of slag aggregation // Republican Scientific and Technical Conference "Modern Problems and Prospects of Chemistry and Chemical-Metallurgical Production". 204.

[38] J.Clara Jeyageetha (2020). Separation of iron oxide nanoparticles from fly ash of thermal power plant and characterization. International Journal of Scientific and Technical Research, 9(4), 1179-1183.

[39] Pan Liu et. al. (2023). Green approach for rare earth element recovery from coal fly ash. Environmental Science & Technology, 57(13), 5414-5423. https://doi.org/10.1021/acs.est.2c09273

[40] Den Bing et. al. (2023). Heavy metal removal from coal fly ash for low carbon Portland cement production. Nature Communications, 14(1), 1432. https://doi.org/10.5281/zenodo.7490153

[41] Mahendra Kumar et al (2019). Valorization of coal fired-fly ash for potential heavy metal recovery. PMC Open Access Repository, 5(10), e02562. 10.1016/j.heliyon.2019.e02562

[42] D. Valeev et. al. (2019). Complex utilisation of Ekibastuz brown coal fly ash: Iron and carbon separation and aluminum extraction. *Journal of Cleaner Production*, 218, 192-201. https://doi.org/10.1016/j.jclepro.2019.01.34

[43] Liu Cui et. al. (2023). Efficient recovery of aluminum, lithium, iron and gallium from coal fly ash leachate via coextraction and stepwise stripping. Resources, Conservation and Recycling, 202, 107380. https://doi.org/10.1016/j.resconrec.2023.107380

[44] Bennet Sam Thomas et. al. (2024). Extraction and separation of rare earth elements from coal and coal fly ash: A review on fundamental understanding and on-going engineering advancments. *Journal of environmental chemical engineering*, 12(3), 112769, https://doi.org/10.1016/j.jece.2024.112769

[45] Virendra Kumar Yadav et. Al. (2020). Advances in methods for recovery of ferrous, alumina, and silica nanoparticles from fly ash waste. Ceramics, 3(3), 384-420. https://doi.org/10.3390/ceramics3030034

[46] Mutalibkhonov S.S. Khojiyev Sh.T. Khudoymuratov SH.J. Riskulov D.D. Improved method of the fire refining of secondary copper-containing materials. Universum: technical sciences: electron scientific journal. May 2025. – № 5(134). – P. 10. – C. 48–54. https://doi:10.32743/UniTech.2025.134.5.20026

[47] Triana T., Brooks G.A. et al (2024). Iron oxide direct reduction and iron nitride formation using ammonia: Review and thermodynamic analysis. Journal of Sustainable Metallurgy, 10, 1428-1445, https://doi.org/10.1007/s40831-024-00860-z

[48] Vu Thi Ngoc Minh et. al (2023). Firing-associated recycling of coal-fired power plant fly ash. Journal of analytical methods in chemistr, 1, 8597376. https://doi.org/10.1155/2023/8597376

[49] Xiaoman Tian et. al. (2025). Recovery of valuable elements from coal fly ash: A review. Environmental reserach, 282, 121928. https://doi.org/10.1016/j.envres.2025.121928

[50] Daniel Fernandez-Gonzales and et., el. Recovery of Copper and magnetite from copper slag using concentrated solar power. *Metallurgical Research & Technology*, 2020;117(4). https://doi.org/10.3390/met11071032

[51] Mauricio Mura and et. el. Leaching of Copper Slags in Sulphuric Acid and Alkaline Glycine Media. *Frontiers in Chemical Engineering*, 2025;7:1613424. https://doi.org/10.3389/fceng.2025.1613424

[52] Vladimir Luganov and et., el. Chemical Enrichment of Nickel Sulfide Ores. *International Journal of Non-Ferrous Metallurgy*, 2016;5(1):1–12. DOI: 10.4236/ijnm.2016.51001